

DNA KINETICS IN MICROFABRICATED DEVICES

Yick Chuen Chan¹, Rosie Ming Sum Ma¹, Maria Carles^{2,3}, Nikolaus J. Sucher^{2,4}, Man Wong⁵ and Yitshak Zohar¹

¹Department of Mechanical Engineering, ²Biotechnology Research Institute, ³Department of Biochemistry,

⁴Department of Biology, ⁵Department of Electrical & Electronic Engineering

Hong Kong University of Science and Technology, Clear Water Bay, Kowloon, Hong Kong

Tel: +852 23587194, Fax: +852 23581543, Email: mezohar@ust.hk

ABSTRACT

The DNA kinetics in micro-capillary electrophoresis is presented. The mobility and diffusion coefficient of 14bp-DNA fragments as a function of concentration in two types of separation sieving matrices, hydroxyethylcellulose (HEC) polymer solution and agarose gel, are extracted through a series of experiments performed in micro-fabricated devices. In addition, the motion of a DNA plug through a miter bend and splitting a plug in a branch are quantitatively characterized. The concept of equivalent length is introduced to quantify the effect of a bend on the DNA plug motion. In a branching system, a simple kinematic relationship was discovered relating the quantity of DNA in each downstream branch to its relative channel cross-sectional area.

INTRODUCTION

Powered by major advances in microfabrication technology, the development of a fully automated lab-on-chip for genetic assays has been attracting major research and commercial interest. In recent years, numerous miniaturized capillary electrophoresis systems with high performance have been designed and fabricated. The majority of those microsystems were fabricated with bonded, bulk micromachined glass substrates with external electrodes [1,2,3]. Although higher voltages can be applied to those microsystems, the heat dissipation problem and large-scale detection systems limited their potential of becoming good candidates for a lab-on-chip.

Although DNA analysis using capillary electrophoresis has been exercised for more than a decade, detailed characterization of the fundamental processes involved in DNA kinetics, such as diffusion or separation, is still lacking. In slab gel electrophoresis, DNA electrophoretic mobility was already well characterized [4], and the mobility of DNA fragments in polymer solutions was also measured [5,6]. However, little has been said about DNA kinetics in microfabricated capillary electrophoresis (MCE) devices. Various designs incorporating bends along the channel were adopted

to minimize the MCE chip size while maintaining a long separation channel [2,3,7]. Thus far, though, the motion of a DNA plug through a bend has been analyzed only qualitatively. Splitting an injection plug into several channels to carry out different tests is another attractive feature. However, the DNA mass fraction injected to each downstream branch is not known. These issues indicate that despite the widespread utilization of micro-capillary electrophoresis, detailed studies of the DNA kinetics in microfabricated devices with various designs are still needed.

Recently, we presented a novel and robust integrated micro-capillary electrophoresis system with feed-through electrodes, fabricated using amorphous-silicon-assisted glass-to-silicon anodic bonding technology [8]. The use of both silicon and glass substrates with integrated circuits facilitates the design of an automated lab-on-chip. In the present work, this microsystem has been used to study DNA kinetics in a variety of microchannels.

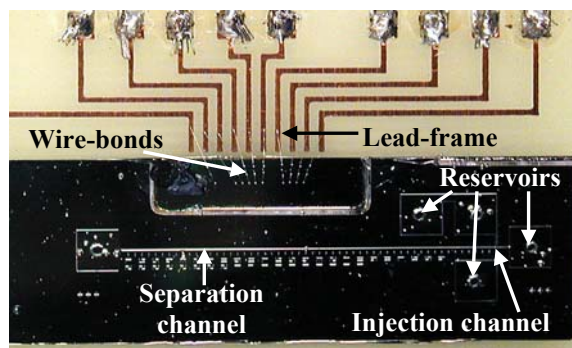


Fig. 1: A picture of a packaged integrated micro-system showing the micro-channels, reservoirs, lead-frame and wire-bonds.

DEVICE DESIGN AND FABRICATION

The detailed design and fabrication of the integrated MCE device is described elsewhere [8]. The injection and separation channels were etched either in a 100mm, Corning 7740 glass wafer or in a 100mm, P-type, (100) Si wafer. Platinum electrodes, with TiW as a glue layer, were sputtered and patterned on a second wafer using the lift off process.

A thick thermal oxide layer was grown on the Si wafer either before the Pt-electrode sputtering (if the channels were etched in the glass wafer) or after channel etching (if the channels were formed in the Si wafer) for electrical insulation. This was followed by the deposition of a very thin amorphous-silicon layer to significantly improve the yield of the glass to oxide anodic bonding. The two processed wafers were then anodically bonded under 900V at 335°C for 1 hour. The process was finally completed with wafer cutting and device packaging. A picture of a packaged device is shown in Figure 1.

Prior to their use, the capillary walls of the fabricated devices were treated using a modified Hjerten procedure [9,10], which consists of a 0.1M NaOH rinsing and a polyacrylamide coating. The NaOH rinsing renders the capillary wall hydrophilic and, hence, facilitates the loading of the sieving matrices. The polyacrylamide coating suppresses electro-osmotic flow (EOF) for the subsequent experiments. This is especially important when using polymer solution, rather than gel, as the sieving matrix because EOF results in a bulk motion of both the sieving matrix and the DNA, which in turn affects the experimental measurements.

EXPERIMENTAL SET-UP

The packaged MCE device was loaded with the appropriate amount of sieving matrix and DNA labeled with FITC, and connected to a voltage divider as described in [8]. Upon the application of an electric field in the injection mode, a pinched DNA plug was obtained. Instantaneous switching to separation mode resulted in a well-defined DNA plug moving into the separation channel. The voltage divider was then disconnected, and direct electric field was applied to the separation channel to conduct the experiments. The experiments were viewed using a CCD camera mounted on a microscope. Image acquisition and analysis software captured the DNA motion. The location and concentration distribution of DNA could then be extracted from the light-intensity distribution observed in the still pictures.

RESULTS AND DISCUSSION

The motion of a DNA plug in a microchannel, under an applied electric field E , is governed by the one-dimensional convective diffusion equation, which admits a normal-distribution solution for the DNA concentration $C(x,t)$ as follows:

$$C(x,t) = \frac{M}{S\sqrt{4\pi Dt}} \exp\left[-\frac{(x-x_m)^2}{4Dt}\right] \quad (1)$$

This equation facilitates the calculation of the mobility, $\mu = x_m/Et$, and diffusion coefficient, $D = \sigma^2/2t$, from the measurements of the time-dependent peak location x_m and standard deviation σ of the DNA distribution in the separation channel. Several images were recorded as the plug travelled along the separation channel, under applied electric field, in either the HEC polymer solution or the agarose gel.

A typical set of velocity measurements of 14bp-DNA fragments as a function of the electric field for different agarose gel concentration is plotted in Figure 2. Indeed, the velocity increases linearly with the electric field strength. The constant slope, which is the mobility, increases with decreasing concentration. The experiments were repeated for HEC, and the extracted mobility is shown in Figure 3 as a function of the concentration of both matrices. The mobility decreases exponentially as the matrix concentration C increases, $\mu = \mu_0 \cdot \exp(-K_r C)$; K_r is known as the retardation coefficient, which is a characteristic of a given molecular species in a particular molecular system. Interpolation of the curves to zero concentration, yields the constant $\mu_0 = 3.7 \cdot 10^{-4}$ and $3.3 \cdot 10^{-4} \text{ cm}^2/\text{V/s}$ for agarose and HEC, respectively, which is the free-solution mobility.

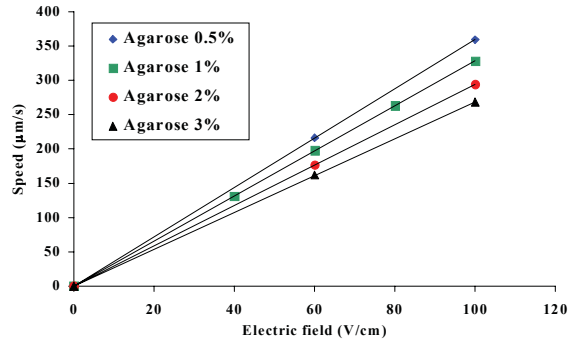


Fig. 2: Plug peak velocity dependence on the electric field for various concentrations of agarose (14bp).

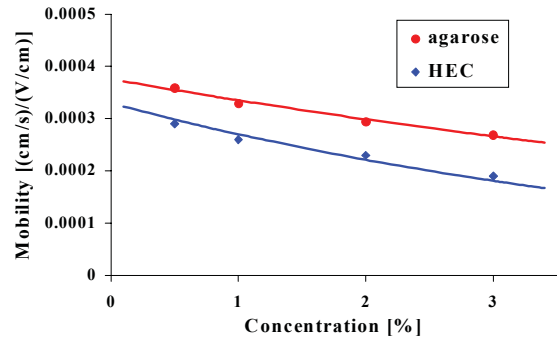


Fig. 3: Mobility dependence on the concentration of the agarose and HEC matrix (14bp).

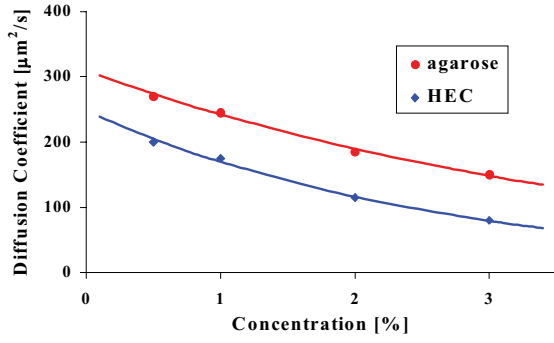


Fig. 4: Diffusion-coefficient dependence on the concentration of the HEC and agarose matrix (14bp).

Another set of experiments was conducted to determine the diffusion coefficient. Similar to the mobility experiments, a DNA plug was injected into the separation channel. However, in this case, the electric field was turned off once the plug cleared the channel intersection. The variance of the DNA distribution in the channel increased linearly with time, and the diffusion coefficient is half the slope. Consistent with the mobility measurements, the estimated diffusion coefficient for agarose is higher than that of HEC as shown in Figure 4 as a function of the matrix concentration.

Several designs have incorporated bends along the channel to lengthen the separation channel without increasing the MCE chip size. However, the motion of a DNA plug around a bend has been analyzed only visually up to now. The plug motion through a miter bend, a sharp turn of 90°, is shown in the picture series in Figure 5, where the DNA distribution is significantly altered due to the bending motion. The concept of equivalent length, L_e , is proposed in order to quantify the effect of the bend on the plug motion and, thus, allow a systematic comparison between the effects of different bends.

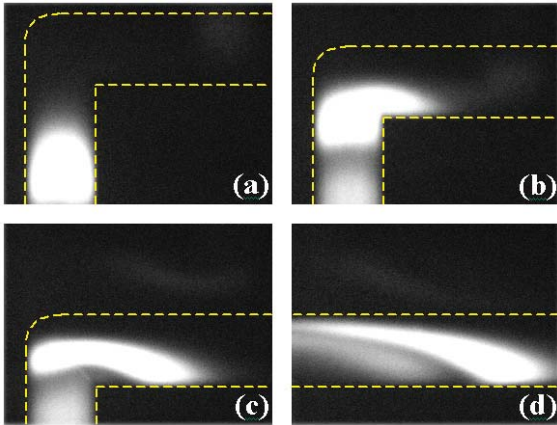


Fig. 5: The DNA plug motion around a bend in the separation channel; the time sequence is a-b-c-d.

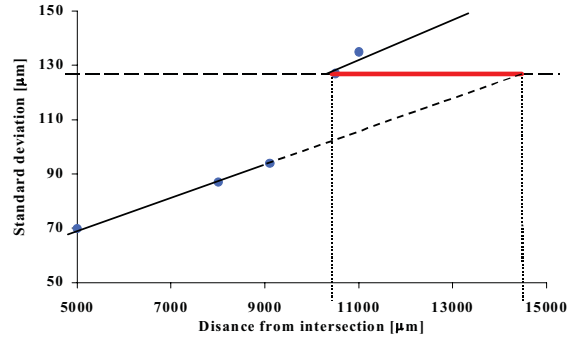


Fig. 6: Evolution of the 14bp-DNA standard deviation as the plug moves through a miter bend, showing the equivalent length, L_e , of the straight channel that would result in the same band broadening as the bend.

In this concept, the band broadening due to the plug motion in a straight microchannel is compared with the band broadening due to the bend. The standard deviation of the DNA concentration, as the plug moves through the miter-bend, is plotted and compared with the standard-deviation evolution along a straight channel in Figure 6. The standard deviation increases linearly with the plug travel distance in the straight section before and after the bend with almost the same slope. The equivalent length of the bend is the length of the straight channel that would result in identical bend-induced band broadening. In this example, this equivalent length of the bend is about 4000 μm. The equivalent length may depend on the arbitrary decision at which location the bend effect is over. This location is the point the band-broadening slope thereafter is equal to the slope before the bend.

In a similar fashion, the effect of various geometrical features, like local contraction or expansion of the separation channel, on the band broadening can be quantified for design purposes.

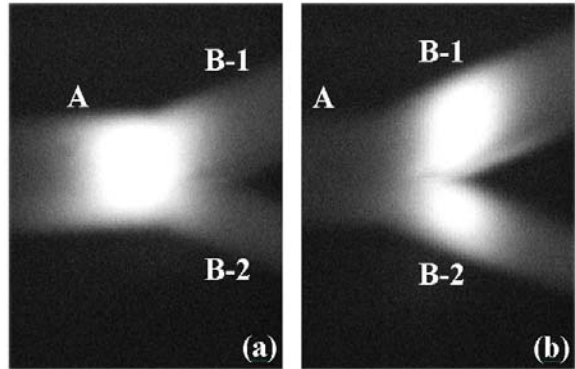


Fig. 7: Plug motion through a branch in the separation channel: (a) upstream and (b) downstream of the branch.

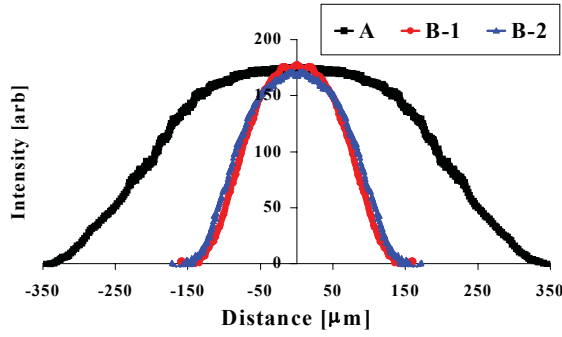


Fig. 8: 14bp-DNA light intensity distributions upstream (A), and downstream (B-1 and B-2) of the branch.

Splitting an injection plug into several channels, as demonstrated in Figure 7, to simultaneously carry out several tests on the same DNA sample is another attractive geometrical feature. However, the mass fraction injected into each downstream branch from the upstream branch is not known. The light intensity distribution, observed in the pictures of Figure 7, is directly proportional to the DNA concentration. Based on these pictures, the light intensity distributions in the upstream branch (A) and the two downstream branches (B-1 & B-2) are plotted in Figure 8. According to Equation 1, the DNA concentration in each straight branch is proportional to the DNA mass per unit cross-section area, M/S . Since these are normal distributions, the area under each curve is directly proportional to the total mass within each branch divided by its cross-section area, M_i/S_i . Conservation of mass requires $M_A = M_{B-1} + M_{B-2}$. Indeed, we found that $S_A A_A = S_{B-1} A_{B-1} + S_{B-2} A_{B-2}$, where A denotes the area under the distribution curve. Furthermore, we discovered that the area under the distribution of each downstream branch is the same, $A_{B-1} = A_{B-2}$. Namely, the average ‘density’ in each downstream branch is the same, $M_{B-1}/S_{B-1} = M_{B-2}/S_{B-2}$. Therefore, at least for the current system of two branches, the DNA mass injected into each downstream branch is proportional to its relative cross-sectional area. A general kinematic relationship for the mass injected into each downstream branch from a single upstream branch can be expressed as:

$$M_j = \frac{\sum_{i=1}^n M_i}{\sum_{i=1}^n S_i} S_j \quad (2)$$

where n is the number of downstream branches. Equation 2 was shown to be valid only for two downstream branches, and more experiments are needed to verify it for more branches.

CONCLUSIONS

Measurements of the diffusion coefficient and mobility of DNA short fragments (14bp) in a microfabricated channel are reported using either agarose or HEC as the sieving matrix. The average free-solution mobility of $3.5 \cdot 10^{-4} \text{ cm}^2/\text{V/s}$ is in good agreement with measurements published in standard electrophoresis systems. The mobility and diffusion coefficient in agarose are higher than those in HEC.

The concept of equivalent length is introduced to quantitatively characterize the plug motion through a miter bend. Using this concept, the effect of various geometric features on band broadening within the separation channel can be evaluated. Finally, a general kinematic relation for predicting the DNA mass fraction injected into several downstream from a single upstream branch is proposed.

ACKNOWLEDGMENTS

This work is supported by the Hong Kong Research Grant Council through RGC grant HKUST6082/00E, the Industry Department of the Hong Kong SAR (AF/150/99) and the Hong Kong Jockey Club.

REFERENCES

- [1] D.J. Harrison, K. Fluri, K. Seiler, Z. Fan, C.S. Effenhauser & A. Manz, *Science*, vol. 261, pp. 895-897, 1993.
- [2] S.C. Jacobson, R. Hergenroder, L.B. Koutny, R.J. Warmack & J.M. Ramsey, *Analytical Chemistry*, vol. 66, pp. 1107-1113, 1994.
- [3] D. Schmalzing, L. Koutny, A. Adourian, P. Belgrader, P. Matsudaira & D. Ehrlich, *Proceedings of the National Academy of Sciences of the United States of America*, vol. 94, pp. 10273-10278, 1997.
- [4] K. Strutz & N.C. Stellwagen, *Electrophoresis*, vol. 19, pp. 635-642, 1998.
- [5] W.M. Sunada & H.W. Blanch, *Electrophoresis*, vol. 19, pp. 3128-3136, 1998.
- [6] A.E. Barron, H.W. Blanch & D.S. Soane, *Electrophoresis*, vol. 15, pp. 597-615, 1994.
- [7] F.E. Regnier, B. He, S. Lin & J. Busse, *Trends in Biotechnology*, vol. 17, pp. 101-106, 1999.
- [8] Y.C. Chan, R. Lenigk, M. Carles, N.J. Sucher, M. Wong & Y. Zohar, *Transducers'01*, pp. 1166-1169, 2001.
- [9] S. Hjerten, *Journal of Chromatography*, vol. 347, pp. 191-198, 1985.
- [10] S. Hjerten & M. Kiessling-Johansson, *Journal of Chromatography*, vol. 550, pp. 811-822, 1991.